Electronic Supplementary Information

A structure-sensitive descriptor for the design of active sites on MoS$_2$ catalysts

*Hai-Yan Su, Federico Calle-Vallejo*, and Keju Sun**

*Corresponding authors. Emails: federico.calle@ehu.es; kjsun@ysu.edu.cn

S1. Assessing *cn*

- When the coverage of vacancies is $\theta = 1/15$ ML (Fig. 1a), Mo_I, Mo_{II} and Mo_{III} coordinate each with 5 S atoms, and each S atom coordinates with 3 Mo atoms. Thus, the number of S atoms coordinated to the Mo_I-Mo_{III} atoms is: $cn = (5 + 5 + 5) \times 1/3 = 5.00$.

- When $\theta = 2/15$ ML (Fig. 1b), Mo_I, Mo_{II} and Mo_{III} coordinate with 5, 4 and 5 S atoms, and each S atom coordinates with 3 Mo atoms. Thus, $cn = (5 + 4 + 5) \times 1/3 = 4.67$.

- When $\theta = 3/15$ ML (Fig. 1c), Mo_I, Mo_{II} and Mo_{III} coordinate with 5, 3 and 5 S atoms, and each S atom coordinates with 3 Mo atoms. Thus, $cn = (5 + 3 + 5) \times 1/3 = 4.33$.

- When $\theta = 4/15$ ML (Fig. 1d), Mo_I, Mo_{II} and Mo_{III} coordinate with 5, 3 and 4 S atoms, and each S atom coordinates with 3 Mo atoms. Thus, $cn = (5 + 3 + 4) \times 1/3 = 4.00$.

- When $\theta = 5/15$ ML (Fig. 1e), Mo_I, Mo_{II} and Mo_{III} coordinate with 5, 3 and 3 S atoms, and each S atom coordinates with 3 Mo atoms. Thus, $cn = (5 + 3 + 3) \times 1/3 = 3.67$.

- When $\theta = 6/15$ ML (Fig. 1f), Mo_I, Mo_{II} and Mo_{III} coordinate with 4, 3 and 3 S atoms, and each S atom coordinates with 3 Mo atoms. Thus, $cn = (4 + 3 + 3) \times 1/3 = 3.33$.

- Finally, when $\theta = 7/15$ML (Fig. 1g), Mo_I, Mo_{II} and Mo_{III} each coordinate with 3 S atoms, and each S atom coordinates with 3 Mo atoms. Thus, $cn = (3 + 3 + 3) \times 1/3 = 3.00$.

S2. Correlations between d-band centers, S vacancy formation energies and adsorption energies
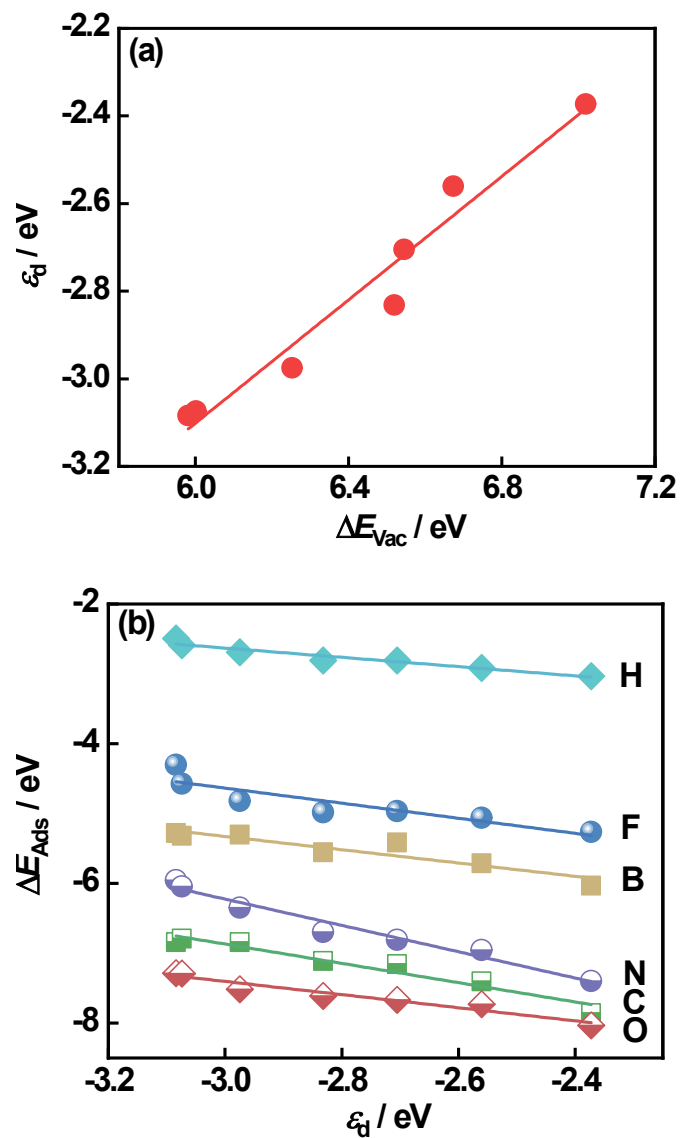
Figure S1. Correlation between the d-band center (ε_d) of the Mo atoms at the S vacancy in MoS$_2$(001) surfaces and (a) S vacancy formation energies (ΔE_{Vac}), and (b) the adsorption energies (ΔE_{Ads}) of various atomic species.

S3. Correlations between cohesive energies, S vacancy formation energies and *cn*
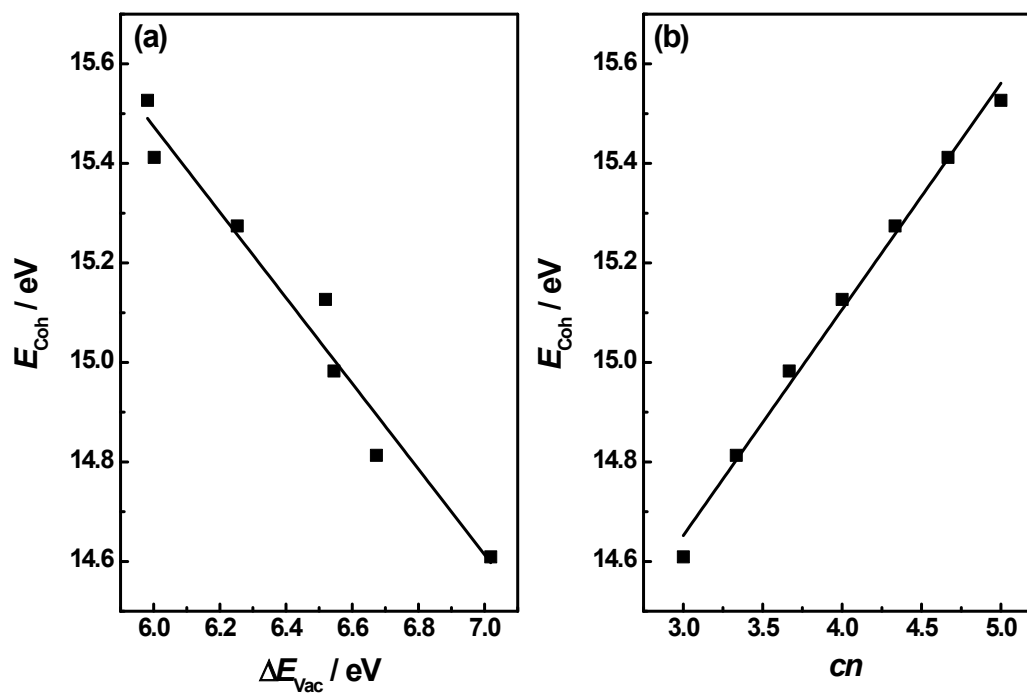
Figure S2. Cohesive energies (E_{Coh} in eV) as a function of (a) S vacancy formation energies (ΔE_{Vac} in eV) and (b) the number of S atoms coordinated to Mo atoms (*cn*) on S-deficient $MoS_2(001)$ surfaces. The data in this figure are tabulated in Tables S1, S2 and S19.

S4. Scaling relation between the adsorption energies of N and other atoms
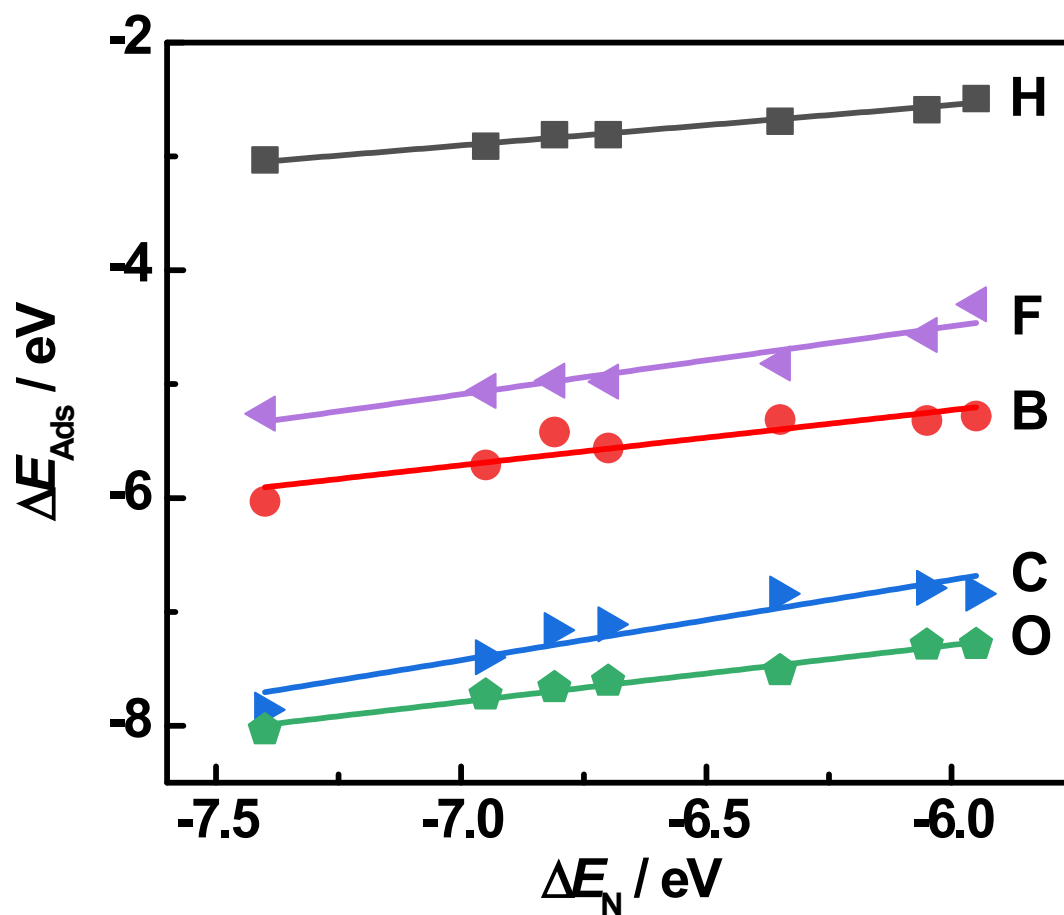
Figure S3. Scaling relation between adsorption energies of *N (ΔE_N) and other atomic species (ΔE_{Ads}).

S5. Differential charge density maps for atomic adsorption
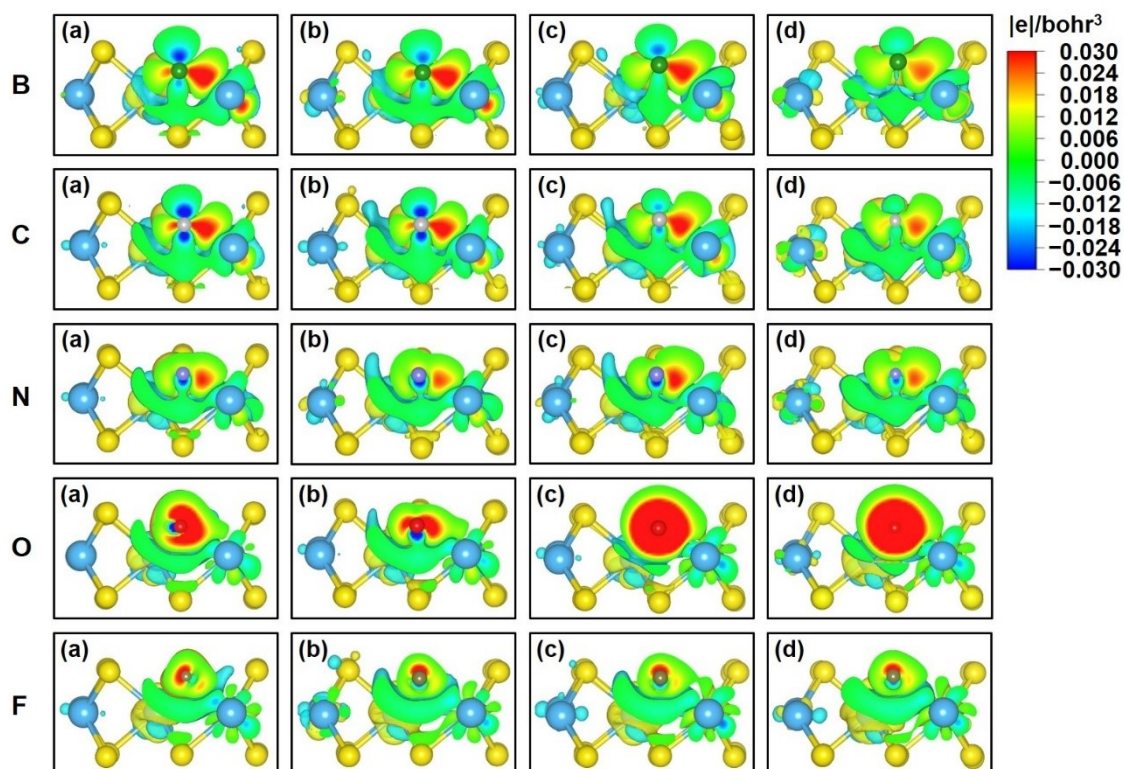
Figure S4. Differential charge density maps for B, C, N, O and F adsorption on MoS$_2$(001) with S vacancy coverages of (a) 1/15, (b) 1/5, (c) 1/3 and (d) 7/15 ML. Blue, yellow, green, gray, purple, red and dark yellow spheres represent Mo, S, B, C, N, O and F, respectively. Blue and yellow-red isosurfaces indicate charge depletion and accumulation. The 2D profile is a cut along a Mo−adsorbate bond.

S6. Transition-state configurations
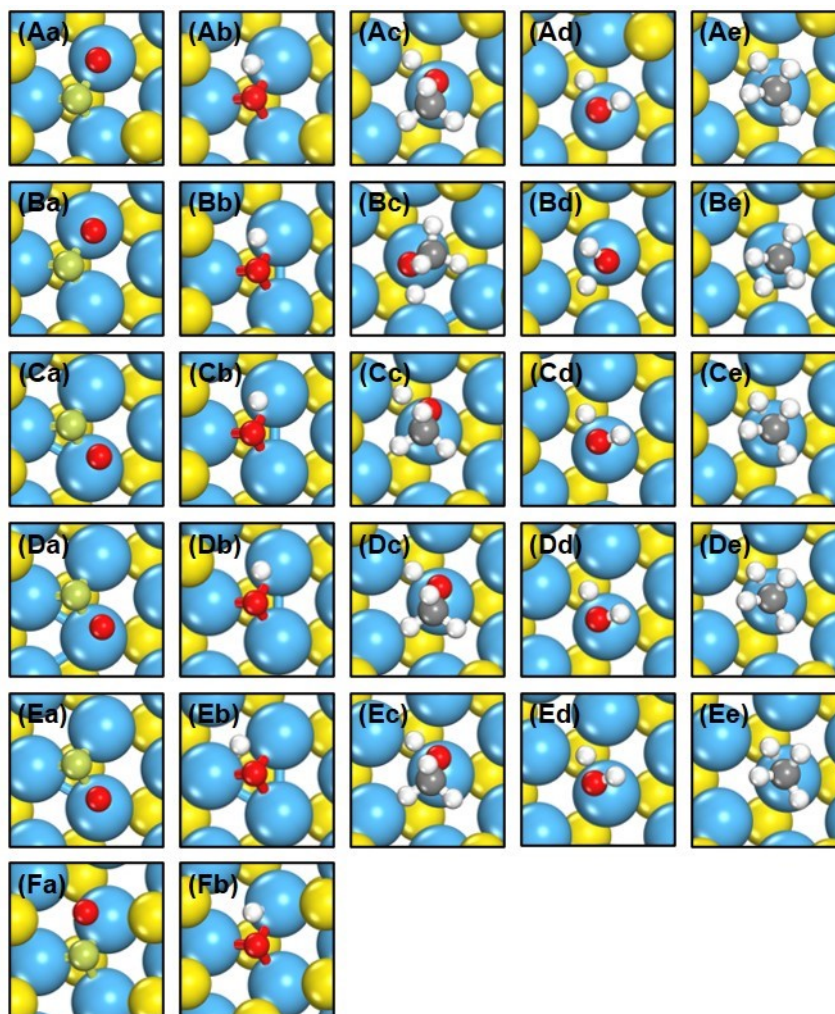
Figure S5. Top views of the transition-state structures of (a) *NO + * → *N + *O, (b) *O + *H → *OH + *, (c) *CH$_3$O + *H → *CH$_3$OH + *, (d) *OH + *H → *H$_2$O + * and (e) *CH$_3$ + *H → CH$_4$ + 2* on MoS$_2$(001) surface with a S vacancy coverage of (A) 1/5, (B) 4/15, (C) 1/3, (D) 2/5, (E) 7/15 and (F) 2/15 ML. Blue, yellow, gray, white, red and green balls represent Mo, S, C, H, O and N atoms, respectively.

S7. Adsorption configurations on Mo edges
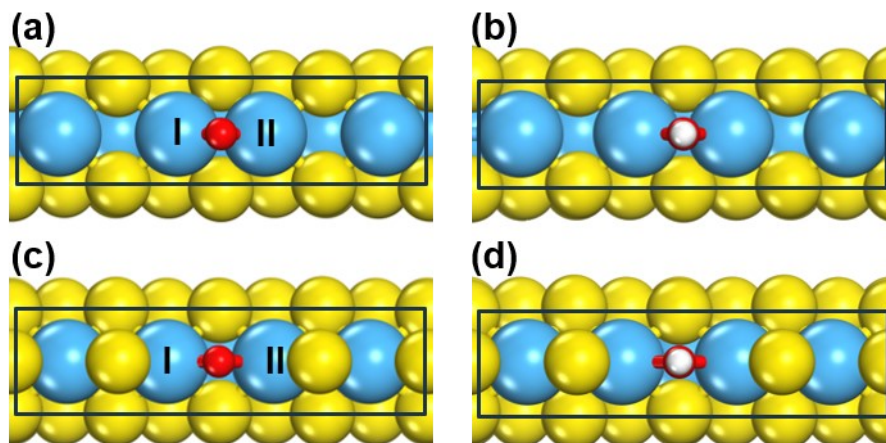
Figure S6. Top view of *O and *OH adsorption on the Mo edge with 100% S vacancy (a, b) and 62.5% S vacancy (c, d). Blue, yellow, red and white balls represent Mo, S, O and H atoms, respectively. The numbers I and II denote the Mo atoms at the S vacancy under study. In (a), Mo_I and Mo_{II} coordinate with four S atoms each, and each S atom coordinates with three Mo atoms, hence: $cn = 4 \times 1/3 \times 2 = 2.67$. In (c), Mo_I and Mo_{II} coordinate with five S atoms, four S atoms among those bind to three Mo atoms, and the remaining S atom binds to two Mo atoms. Thus, $cn = (4 \times 1/3 + 1/2) \times 2 = 3.67$.

S8. Adjacent and far S vacancy configurations
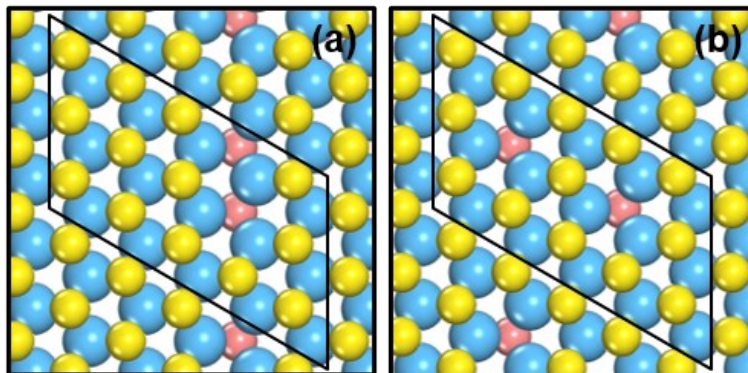
Figure S7. Top view of $MoS_2(001)$ with adjacent (a) and far (b) S vacancy arrangements at 2/15ML vacancy coverages. Blue, yellow and vermilion balls represent Mo, upper S and lower S, respectively.

S9. Data, correlations and associated errors

In the following, the correlations are given as: $y = slope \cdot x + intercept$. For instance, from the first line of Table S2 we have that the correlation of cn vs ΔE_{Vac} is: $cn = -1.88 \, \Delta E_{Vac} + 16.06$.

Cohesive energies are defined as: $E_{Coh} = (x E_{Mo} + y E_S - E_{Mo_x S_y})/x$. Our calculated cohesive energy for pristine MoS$_2$(001) is 15.58 eV, which is close to the widely accepted value (15.55 eV) in the literature by Ataca and Ciraci, found with PW91.[1]

Table S1. Values of the descriptors for the MoS$_2$(001) surfaces as a function of the coverage of S vacancies. ΔE_{Vac}, Φ, E_{Coh} and ε_d in eV, excess Bader charge (BC) in the adsorbates and integrated $coop$ in e$^-$, integrated $cohp$ in eV.

variable	1/15ML	2/15ML	1/5ML	4/15ML	1/3ML	2/5ML	7/15ML
ΔE_{Vac}	5.98	6.00	6.25	6.52	6.54	6.67	7.02
cn	5.00	4.67	4.33	4.00	3.67	3.33	3.00
Φ	5.77	5.69	5.59	5.52	5.47	5.39	5.30
BC_H	-0.33	-0.34	-0.35	-0.37	-0.37	-0.39	-0.41
BC_B	-0.18	-0.20	-0.23	-0.25	-0.39	-0.47	-0.52
BC_C	-0.71	-0.73	-0.77	-0.83	-0.85	-0.89	-0.93
BC_N	-0.92	-0.94	-0.96	-0.98	-1.00	-1.02	-1.04
BC_O	-0.90	-0.91	-0.92	-0.92	-0.93	-0.94	-0.96
BC_F	-0.66	-0.66	-0.67	-0.67	-0.67	-0.68	-0.69
$coop_H$	0.24	0.24	0.23	0.24	0.22	0.23	0.23
$coop_B$	0.71	0.70	0.71	0.70	0.70	0.71	0.74
$coop_C$	0.75	0.76	0.77	0.77	0.76	0.76	0.78
$coop_N$	0.62	0.63	0.63	0.64	0.63	0.63	0.64
$coop_O$	0.38	0.39	0.39	0.40	0.39	0.40	0.40
$coop_F$	0.12	0.14	0.14	0.14	0.14	0.14	0.15
$cohp_H$	-3.54	-3.57	-3.59	-3.62	-3.71	-3.72	-3.72
$cohp_B$	-10.07	-10.10	-10.09	-10.06	-9.90	-9.57	-9.85
$cohp_C$	-12.84	-12.84	-12.95	-13.00	-12.99	-13.00	-13.16
$cohp_N$	-12.79	-12.89	-12.93	-13.13	-13.19	-13.30	-13.55
$cohp_O$	-9.86	-9.96	-10.11	-10.18	-10.28	-10.39	-10.58
$cohp_F$	-4.82	-5.26	-5.16	-5.22	-5.28	-5.27	-5.25
E_{Coh}	15.53	15.41	15.27	15.13	14.98	14.81	14.61
ε_d	-3.08	-3.07	-2.98	-2.83	-2.70	-2.56	-2.37

Table S2. Correlations between ΔE_{Vac} (x) and all properties (y). r, MAE and MAX are the correlation coefficient, mean absolute error (in eV) and maximum absolute error (in eV), respectively.

variables	intercept	slope	r	MAE	MAX
cn	16.06	-1.88	0.97	0.13	0.21
Φ	8.29	-0.43	0.98	0.03	0.04
BC_H	0.09	-0.07	0.99	0.00	0.01
BC_B	1.85	-0.34	0.90	0.04	0.10
BC_C	0.59	-0.22	0.99	0.01	0.02
BC_N	-0.24	-0.11	0.99	0.01	0.01
BC_O	-0.57	-0.05	0.98	0.00	0.01
BC_F	-0.48	-0.03	0.97	0.00	0.01
$coop_H$	0.32	-0.01	0.45	0.00	0.01
$coop_B$	0.58	0.02	0.45	0.01	0.02
$coop_C$	0.65	0.02	0.70	0.01	0.01
$coop_N$	0.54	0.01	0.77	0.00	0.01
$coop_O$	0.29	0.02	0.93	0.00	0.01
$coop_F$	0.02	0.02	0.57	0.00	0.01
$cohp_H$	-2.46	-0.18	0.88	0.03	0.05
$cohp_B$	-12.15	0.34	0.57	0.10	0.29
$cohp_C$	-11.11	-0.29	0.97	0.02	0.03
$cohp_N$	-8.64	-0.70	0.98	0.03	0.08
$cohp_O$	-6.03	-0.65	0.98	0.03	0.08
$cohp_F$	-3.61	-0.24	0.43	0.09	0.25
E_{Coh}	20.64	-0.86	0.98	0.05	0.10
ε_d	-7.33	0.70	0.97	0.04	0.10

Table S3. Adsorption energies (in eV) on MoS$_2$(001) as a function of the coverage of S vacancies.

ΔE_{Ads}	1/15ML	2/15ML	1/5ML	4/15ML	1/3ML	2/5ML	7/15ML
ΔE_H	-2.49	-2.59	-2.69	-2.81	-2.81	-2.91	-3.03
ΔE_B	-5.28	-5.32	-5.31	-5.56	-5.42	-5.71	-6.03
ΔE_C	-6.84	-6.79	-6.84	-7.11	-7.16	-7.40	-7.86
ΔE_N	-5.95	-6.05	-6.35	-6.70	-6.81	-6.95	-7.40
ΔE_O	-7.29	-7.29	-7.52	-7.61	-7.67	-7.73	-8.04
ΔE_F	-4.30	-4.57	-4.82	-4.98	-4.97	-5.06	-5.26
ΔE_{CO}	-0.88	-0.89	-1.86	-1.69	-1.69	-1.95	-2.29
ΔE_{NO}	-2.39	-2.52	-3.20	-3.46	-3.49	-3.61	-3.90
ΔE_{SH}	-2.70	-3.10	-3.49	-3.83	-3.90	-4.04	-4.31
ΔE_{OH}	-3.75	-4.25	-4.46	-4.62	-4.56	-4.64	-4.78
ΔE_{CH}	-6.54	-6.65	-6.81	-6.97	-7.03	-7.11	-7.44
ΔE_{CH3}	-0.91	-1.38	-1.87	-2.36	-2.45	-2.69	-3.02
ΔE_{NH2}	-2.85	-2.94	-3.19	-3.43	-3.38	-3.51	-3.74
ΔE_{CH2}	-4.46	-4.58	-4.79	-4.90	-4.98	-5.02	-5.33

ΔE_{CNH2}	-4.14	-4.22	-4.90	-5.01	-5.00	-5.11	-5.30
ΔE_{CCH3}	-5.37	-5.51	-5.95	-6.11	-6.13	-6.22	-6.50

Table S4. Correlations between all descriptors (*x*) and hydrogen adsorption energies (*y*).

descriptor	intercept	slope	r	MAE	MAX
ΔE_{Vac}	0.37	-0.49	0.98	0.02	0.05
cn	-3.78	0.25	0.99	0.02	0.05
Φ	-9.02	1.13	0.99	0.01	0.03
BC	-0.28	6.77	0.98	0.02	0.05
coop	-6.00	13.81	0.49	0.12	0.27
cohp	5.27	2.21	0.89	0.06	0.11
ε_d	-4.62	-0.66	0.96	0.04	0.08

Table S5. Correlations between all descriptors (*x*) and boron adsorption energies (*y*).

descriptor	intercept	slope	r	MAE	MAX
ΔE_{Vac}	-1.16	-0.68	0.91	0.08	0.18
cn	-6.87	0.34	0.86	0.10	0.21
Φ	-13.81	1.50	0.86	0.10	0.19
BC	-4.96	1.74	0.84	0.10	0.22
coop	4.73	-14.41	0.64	0.15	0.28
cohp	-14.43	-0.90	0.53	0.16	0.43
ε_d	-8.18	-0.95	0.92	0.08	0.19

Table S6. Correlations between all descriptors (*x*) and carbon adsorption energies (*y*).

descriptor	intercept	slope	r	MAE	MAX
ΔE_{Vac}	-0.90	-0.97	0.94	0.10	0.14
cn	-9.10	0.49	0.90	0.12	0.22
Φ	-19.04	2.15	0.90	0.12	0.22
BC	-3.61	4.33	0.92	0.11	0.21
coop	13.55	-27.03	0.54	0.22	0.45
cohp	34.49	3.21	0.91	0.12	0.24
ε_d	-11.01	-1.38	0.97	0.07	0.12

Table S7. Correlations between all descriptors (*x*) and nitrogen adsorption energies (*y*).

descriptor	intercept	slope	r	MAE	MAX
ΔE_{Vac}	2.25	-1.38	1.00	0.03	0.05
cn	-9.43	0.71	0.98	0.07	0.12
Φ	-23.93	3.13	0.99	0.06	0.09
BC	4.97	11.81	0.99	0.05	0.06
coop	32.40	-61.73	0.74	0.27	0.49
cohp	18.76	1.93	0.99	0.06	0.12
ε_d	-11.88	-1.88	0.98	0.07	0.15

Table S8. Correlations between all descriptors (x) and oxygen adsorption energies (y).

descriptor	intercept	slope	r	MAE	MAX
ΔE_{Vac}	-3.15	-0.69	0.99	0.02	0.05
cn	-8.99	0.35	0.96	0.06	0.09
Φ	-16.22	1.56	0.97	0.05	0.08
BC	3.73	12.21	0.98	0.04	0.07
$coop$	7.01	-37.19	0.92	0.07	0.13
$cohp$	3.02	1.04	0.98	0.04	0.07
ε_d	-10.23	-0.94	0.97	0.05	0.09

Table S9. Correlations between all descriptors (x) and fluorine adsorption energies (y).

descriptor	intercept	slope	r	MAE	MAX
ΔE_{Vac}	0.41	-0.82	0.94	0.07	0.19
cn	-6.57	0.43	0.95	0.07	0.13
Φ	-15.48	1.92	0.97	0.06	0.11
BC	12.96	26.58	0.93	0.08	0.18
$coop$	-1.29	-25.53	0.82	0.12	0.29
$cohp$	2.93	1.50	0.70	0.13	0.40
ε_d	-7.87	-1.08	0.88	0.10	0.24

Table S10. Averages (in eV) per descriptor of the mean absolute errors in Tables S4-S9.

descriptor	overall MAE
ΔE_{Vac}	0.06
cn	0.07
Φ	0.07
BC	0.07
$coop$	0.16
$cohp$	0.10
ε_d	0.07

Table S11. Correlations between ΔE_{Vac} (x) and adsorption energies of diatomic species (y).

species	intercept	slope	r	MAE	MAX
ΔE_{CO}	6.69	-1.29	0.89	0.14	0.48
ΔE_{NO}	6.11	-1.45	0.95	0.13	0.23
ΔE_{SH}	5.67	-1.45	0.95	0.13	0.28
ΔE_{OH}	0.65	-0.79	0.82	0.13	0.34
ΔE_{CH}	-1.83	-0.80	0.99	0.03	0.06
Average				0.11	

Table S12. Correlations between cn (x) and adsorption energies of diatomic species (y).

species	intercept	slope	r	MAE	MAX
ΔE_{CO}	-4.25	0.66	0.87	0.16	0.48
ΔE_{NO}	-6.22	0.75	0.94	0.14	0.24
ΔE_{SH}	-6.68	0.76	0.97	0.10	0.21
ΔE_{OH}	-6.15	0.43	0.86	0.13	0.27
ΔE_{CH}	-8.57	0.41	0.98	0.04	0.10
Average				0.11	

Table S13. Correlations between ΔE_{Vac} (x) and adsorption energies of multiatomic species (y).

species	intercept	slope	r	MAE	MAX
ΔE_{CH3}	10.31	-1.93	0.96	0.15	0.32
ΔE_{NH2}	2.06	-0.83	0.99	0.03	0.07
ΔE_{CH2}	0.08	-0.77	0.99	0.04	0.07
ΔE_{CNH2}	2.33	-1.11	0.91	0.13	0.28
ΔE_{CCH3}	0.69	-1.04	0.97	0.07	0.16
Average				0.09	

Table S14. Correlations between cn (x) and adsorption energies of multiatomic species (y).

species	intercept	slope	r	MAE	MAX
ΔE_{CH3}	-6.17	1.02	0.98	0.11	0.26
ΔE_{NH2}	-5.00	0.43	0.97	0.06	0.13
ΔE_{CH2}	-6.45	0.40	0.97	0.05	0.11
ΔE_{CNH2}	-7.10	0.57	0.90	0.14	0.28
ΔE_{CCH3}	-8.11	0.53	0.96	0.08	0.15
Average				0.09	

Table S15. Reaction energies (ΔH, in eV) and activation energies (ΔE_{Act}, in eV) of various elementary reactions on the MoS$_2$(001) surfaces as a function of the coverage of S vacancies.

reaction		2/15ML	1/5ML	4/15ML	1/3ML	2/5ML	7/15ML
*O + *H → *OH + *	ΔH	0.74	0.86	0.91	1.02	1.12	1.40
	ΔE_{Act}	1.78	1.96	2.02	2.03	2.08	2.10
*CH$_3$O + *H → *CH$_3$OH + *	ΔH		0.78	1.03	1.00	1.19	1.55
	ΔE_{Act}		1.73	1.99	1.82	2.01	2.24
*OH + *H → *H$_2$O + *	ΔH		0.68	1.00	0.89	1.11	1.39
	ΔE_{Act}		1.69	1.91	1.86	1.97	2.13
*CH$_3$ + *H → CH$_4$ + 2*	ΔH		-0.15	0.45	0.54	0.88	1.33
	ΔE_{Act}		0.59	1.03	1.15	1.38	1.79
*NO + * → *N + *O	ΔH	-3.24	-3.08	-3.26	-3.41	-3.50	-3.95
	ΔE_{Act}	1.01	0.77	0.68	0.59	0.55	0.45

Table S16. Correlations between *cn* (*x*) and reaction energies (ΔH) and activation energies (ΔE_{Act}) (*y*) for various elementary reactions.

reaction		intercept	slope	r	MAE	MAX
*O + *H → *OH + *	ΔH	2.37	-0.36	0.95	0.05	0.09
	ΔE_{Act}	2.65	-0.17	0.87	0.04	0.08
*CH$_3$O + *H → *CH$_3$OH + *	ΔH	2.98	-0.51	0.92	0.08	0.11
	ΔE_{Act}	3.10	-0.31	0.78	0.08	0.14
*OH + *H → *H$_2$O + *	ΔH	2.70	-0.46	0.89	0.08	0.14
	ΔE_{Act}	2.95	-0.28	0.90	0.05	0.09
*CH$_3$ + *H → CH$_4$ + 2*	ΔH	4.34	-1.02	0.97	0.09	0.18
	ΔE_{Act}	4.21	-0.83	0.98	0.07	0.12
*NO + * → *N + *O	ΔH	-5.03	0.42	0.84	0.13	0.19
	ΔE_{Act}	-0.50	0.31	0.95	0.05	0.08

Table S17. Number of S atoms coordinated to Mo atoms (*cn*) and adsorption energies (ΔE_{Ads}, in eV) of *O and *OH at the S vacancy (S$_v$) on the Mo edge with different S vacancy (S$_v$) arrangement.

description	*cn*	ΔE_{Ads}(O)	ΔE_{Ads}(OH)
Mo edge-100% S$_v$	2.67	-7.95	-5.12
Mo edge-62.5% S$_v$	3.67	-5.56	-4.27

Table S18. Adsorption energies (ΔE_{Ads}, in eV) of species at favorable adsorption sites on a S edge with 50% S vacancy (S$_v$) coverage and a Mo edge with 62.5% S$_v$ coverage. ΔE_{Ads} of H is calculated with respect to 1/2H$_2$ in gas phase. Data taken from Appl. Surf. Sci. 2023, 635, 157721.

species	S edge (*cn* = 3.33)	Mo edge (*cn* = 3.67)
H	-0.19	-0.31
CO	-0.67	-1.08
O	-5.41	-5.56
OH	-3.41	-4.27
CHO	-1.84	-2.16
CH$_2$O	-0.28	-0.94
CH$_3$O	-2.68	-3.34
CH$_2$OH	-1.31	-2.12
HCOO	-2.74	-3.15
COOH	-2.02	-2.54
CH$_3$	-1.43	-1.77

Table S19. Correlation between the number of S atoms coordinated to Mo atoms *cn* (*x*) and cohesive energies E_{Coh} (*y*) in eV.

intercept	slope	r	MAE	MAX
13.29	0.45	1.00	0.02	0.04

S10. Electrocatalytic modelling

We employed the microkinetic model by Nørskov et al to estimate the HER exchange current densities (i_0).[2] In this model, the left leg of the activity plot, for catalysts with $\Delta G_H < 0$, is given by:

$$i_0 = \frac{-ec \cdot k_0}{1 + e^{-\Delta G_H/k_B T}}$$

(S1)

In Equation S1 $-ec = 1.602 \cdot 10^{-19} C$ is the charge of an electron, T is the absolute temperature and was set to 300 K, $k_B = 8.617 \cdot 10^{-5} eV \ K^{-1}$ is the Boltzmann constant, and k_0 is a free parameter in the model used to provide exchange current densities of similar magnitude as the experimental ones but has no influence on the activity trends. In this case, we used a value of $2 \cdot 10^{15} s^{-1} cm^{-2}$, which gives exchange current densities around the apex of the activity plot close to $40 \ \mu A \ cm^{-2}$, in line with those in previous works.[3] Furthermore, the right leg of the activity plot, where catalysts display $\Delta G_H > 0$, the exchange current density is given by:

$$i_0 = \frac{-ec \cdot k_0 \cdot e^{-\Delta G_H/k_B T}}{1 + e^{-\Delta G_H/k_B T}}$$

(S2)

The free energy of adsorption of hydrogen was calculated as $\Delta G_H = \Delta E_H^{DFT} + \Delta ZPE - T\Delta S + xcc$. In this equation, $\Delta E_H^{DFT} = E_{*H} - E_* - \frac{1}{2}E_{H_2}$ is the binding energy of hydrogen, calculated by changing the scale of the values in Table S3; ΔZPE is the zero-point energy change ($ZPE_{*H} = 0.15 \ eV$, $ZPE_{H_2} = 0.27 \ eV$); $T\Delta S$ is the entropic contribution to the free energy ($TS_{*H} = 0.01 \ eV$, $TS_{H_2} = 0.40 \ eV$); and xcc is an exchange-correlation correction necessary here because the calculations of Nørskov et al were made with RPBE and ours with PBE, and PBE usually provides stronger adsorption energies

than RPBE $xcc = 0.17\ eV$. This value is calculated as the difference between the adsorption energy of *H on Pt(111) using PBE (-0.26 eV) and RPBE (-0.09 eV).[2] As experiments have shown that Pt(111) binds *H too strongly by ~0.1 eV,[4] the RPBE-calculated adsorption energy is presumably more accurate in this case.

For completeness, we ought to mention that there are some criticisms to Nørskov et al's microkinetic model in the literature.[5-8] Interested readers are kindly advised to read the cited references.

S11. References

1.   Ataca, C.; Ciraci, S. Functionalization of Single-Layer MoS_2 Honeycomb Structures. *J. Phys. Chem. C* **2011**, *115*, 13303–13311.

2.   Nørskov, J. K.; Bligaard, T.; Logadottir, A.; Kitchin, J. R.; Chen, J. G.; Pandelov, S.; Stimming, U. Trends in the Exchange Current for Hydrogen Evolution. *J. Electrochem. Soc.* **2005**, *152*, J23.

3.   Li, H.; Tsai, C.; Koh, A. L.; Cai, L.; Contryman, A. W.; Fragapane, A. H.; Zhao, J.; Han, H. S.; Manoharan, H. C.; Abild-Pedersen, F.; Norskov, J. K.; Zheng, X. Activating and Optimizing MoS_2 Basal Planes for Hydrogen Evolution through the Formation of Strained Sulphur Vacancies. *Nat. Mater.* **2016**, *15*, 48–53.

4.   Pohl, M. D.; Watzele, S.; Calle-Vallejo, F.; Bandarenka, A. S. Nature of Highly Active Electrocatalytic Sites for the Hydrogen Evolution Reaction at Pt Electrodes in Acidic Media. *ACS Omega* **2017**, *2*, 8141−8147.

5.   Quaino, P.; Juarez, F.; Santos, E.; Schmickler, W. Volcano Plots in Hydrogen Electrocatalysis–Uses and Abuses. *Beilstein J. Nanotech.* **2014**, *5*, 846–854.

6.   Zeradjanin, A. R.; Grote, J. -P.; Polymeros, G.; Mayhofer, K. J. J. A Critical Review on Hydrogen Evolution Electrocatalysis: Re–Exploring the Volcano–Relationship. *Electroanal.* **2016**, *28*, 2256–2269.

7.   Lindgren, P.; Kastlunger, G.; Peterson, A. A. A Challenge to the G similar to 0 Interpretation of Hydrogen Evolution. *ACS Catal.* **2020**, *10*, 121–128.

8.   Exner, K. S. Does a Thermoneutral Electrocatalyst Correspond to the Apex of a Volcano Plot for a Simple Two-Electron Process? *Angew. Chem. Int. Ed.* **2020***, 132*, 10320–10324.